

SUBSURFACE WATER ICE MAPPING (SWIM) ON MARS: PLANET-WIDE GEOMORPHIC MAPPING OF ICE-RELATED LANDFORMS. D.M.H. Baker¹, G.A. Morgan², A. Pathare², C.M. Dundas³, N.E. Putzig², and the SWIM Team. ¹NASA Goddard Space Flight Center, Greenbelt, MD (david.m.hollibaughbaker@nasa.gov), ²Planetary Science Institute, ³U.S. Geological Survey.

Introduction: The Subsurface Water Ice Mapping (SWIM) project supports an effort by NASA's Mars Exploration Program to determine *in situ* resource availability [1-2]. Since 2019, the project has been performing global reconnaissance and multi-dataset mapping to characterize the distribution of water ice from 60°S to 60°N [1-2]. In 2019, we produced "ice consistency" maps (quantitative assessment of how consistent or inconsistent the various datasets are with the presence of buried water ice) for the northern hemisphere (0–60°N) from 0–225°E and 290–360°E. In 2020, we extended our mapping into the southern hemisphere (0–60°S) and from 225–290°E in the northern hemisphere at elevations <+1 km. Our combined maps have been made available on the SWIM project website (<https://swim.psi.edu>).

Here and in additional abstracts presented at this conference [3,4], we report on current efforts to refine the geomorphic mapping of periglacial and glacial features on Mars. Geomorphology is an important input to the SWIM ice consistency maps, as specific landforms can be used to infer ice presence over a range of depths, and can be observed directly from imagery over a near-continuous spatial extent within the study area. Importantly, we are focused on the *present* locations of ice and therefore are mapping landforms that have the highest potential for indicating ice at depth. These landforms are distinct from the many erosional and depositional landforms that exist on Mars that may indicate the *past* presence of ice.

Mapping Methods: Our previous SWIM geomorphology work used grid mapping methods [5] at variable resolutions (i.e., grid cell sizes) to survey periglacial and glacial landforms across the northern and southern hemisphere of Mars. These landforms are tallied and variously weighted to produce geomorphology ice consistency values for each grid cell. For simplicity, here we will define geomorphology "ice consistency" as the normalized sum of all landforms mapped within a grid cell. We have been using the CTX image mosaic (beta01 version) at 6 m/pixel resolution produced by the Caltech Murray Lab [6] as our primary basemap.

Prior Mapping Methods: Our northern hemisphere mapping (SWIM 2019 products) was based on previous [7-8] and new mapping of the presence of periglacial and

glacial landforms. A sampling of 4x4° sized CTX image mosaics within previously mapped geologic units [9] was used to tally the number of observed landforms and to extrapolate the observations to the geologic unit boundaries.

We improved the grid-mapping methods in the southern hemisphere (SWIM 2020 products) by completely mapping landforms observed within the global CTX mosaic at grid cell sizes of 4x4° across regions <+1 km in elevation. To better define the equatorward boundary of ice-related landforms, we improved this mapping resolution to 1x1° in the 24–38°S latitude range. The 1x1° scale (~60 km at the equator) was chosen for mapping efficiency and to be less than the scale of a human exploration zone (100 km radius) [10].

Updated Methods (Northern Hemisphere): To improve the definition of the boundaries of ice-related features in the northern hemisphere, including their equatorward extent, and to make the mapping more consistent with that in the southern hemisphere, we are currently increasing mapping resolution to 4x4° continuously from 16–40°N. We are also refining the equatorward boundary of ice-rich landforms with 1x1° mapping over a 10° wide latitude zone.

Combined Global Mapping Results: Our combined SWIM results (**Fig. 1**) show much refinement to our understanding of the spatial extent and locations of periglacial and glacial landforms on Mars. Our current 4x4° and 1x1° mapping in the northern hemisphere (**Fig. 1** grid cells) show considerable improvement in the delineation of features within 16–40°N over the previous SWIM map products.

The broad-scale, latitude-dependent trends of periglacial and glacial landforms are generally consistent with previous studies [e.g., 11], with the greatest concentration of ice-rich landforms located between ~35° and 55° latitude in both hemispheres (**Fig. 1**). Areas with the highest concentration of landforms occur in Arcadia and Utopia Planitiae, Tempe Terra (northern hemisphere) and Hellas Planitia (southern hemisphere) (**Fig. 1**). The equatorward extent of landforms is variable around the 30° latitude lines with the greatest equatorward excursions to ~20–24°N occurring in regions of high topography in Arabia Terra and the northern Tharsis rise. Interestingly, the most frequent

equatorward excursions within our survey in the southern hemisphere occur within the low altitudes of Hellas Planitia. The smaller number of landforms from 50° to 60°N leading to lower ice consistency values may simply indicate that ice-related geomorphology is less diverse there, possibly because of reduced ablation (and thus related landform development) at these higher latitudes.

While some correlation between specific landforms exists, there are large variations in both local concentrations and equatorward extent. For example, mantle units of varying morphology are widespread and extend to low latitudes where units are generally patchy and dissected. Glacial features (i.e., lobate debris aprons, lineated valley fill, and concentric crater fill [7]) are also widespread and occur at low latitudes, but they are concentrated in regions with abundant topographic slopes that likely enabled ice accumulation and are confined to craters at the lowest latitudes. Scalloped terrain is highly restricted to specific regions with mantle or other ice-rich units, including those in Utopia, Arcadia, and Hellas Planitiae, and they generally do not occur below ~40° latitude.

Lowest Latitude Landforms: Identifying the lowest latitude (<30°) sites with available and accessible ice is of particular interest for human exploration to reduce risk and complexity of surface operations (e.g., higher insolation and temperatures) and to supply fuel for the return to Earth. Based on our mapping, the types and morphological character of landforms present at the lowest latitudes are distinct from those at the highest latitudes in several ways: 1) they are sparser in number, 2) they are more restricted in type, generally to mantle,

CCF, or “icy” crater fill material, and 3) they occur in more isolated and less accessible locations, mainly on pole-facing slopes and/or confined to craters.

Intriguingly, we identify near-equatorial ice-like landforms centered at 5°S, 10°E (see cluster of blue pixels at this location in **Fig. 1**), coinciding with observations of glacial-like landforms by [12]. In addition, we observe mantle-type units at this location with sublimation-like pits and textures.

Future Work: We are continuing mapping in the northern hemisphere and will combine the results of ongoing HiRISE observations of thermal-contraction crack polygons in the midlatitudes [4]. We anticipate presenting more complete maps and concluding this effort by Summer 2022.

Acknowledgments: The SWIM project is supported by NASA through JPL Subcontracts 1611855, 1639821, and 1670015. Thanks to the Caltech Murray Lab for making the CTX mosaics publicly available (<http://murray-lab.caltech.edu/CTX/>).

References: [1] Morgan, G.A. et al. (2021) *Nature Astronomy* 5, 230–236. [2] Putzig, N.E. et al. (in press) Ch. 16 of Badescu et al., eds., *Handbook of Space Resources*, Springer. [3] Putzig, N.E. et al. (2022) *LPSC 53* (this conference). [4] Morgan, G.A. et al. (2022) *LPSC 53* (this conference). [5] Ramsdale, J.D. et al. (2017) *PSS* 140, 49–61. [6] Dickson, J.L. et al. (2018) *LPSC 49*, 2480. [7] Levy J. et al. (2014) *JGR* 119, 2188–2196. [8] Kadish, S.J. et al. (2009) *JGR* 114, E10001. [9] Tanaka, K.L. et al. (2005) *USGS SIM* 2888. [10] Beaty, D. et al. (2015) *HLS2 Workshop*, <https://www.nasa.gov/feature/mars-human-landing-site-workshop-presentations/>. [11] Milliken R.E. et al. (2003) *JGR* 108, E6, 5057. [12] Shean, D.E. (2010) *GRL* 37, L24202.

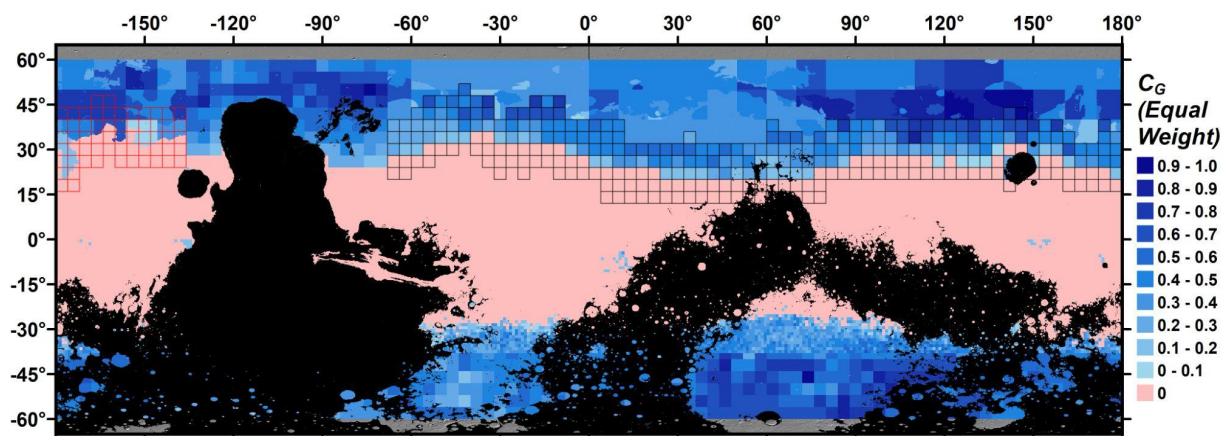


Fig. 1. SWIM geomorphology (C_G) “ice consistency” map with MOLA elevations >+1km masked in black. Blue shades indicate presence of periglacial or glacial landforms and the pink color indicates no observed landforms. Black grid cells at 4x4° in size in the northern hemisphere show current progress in improving delineation of the equatorward extent of ice-related landforms. Red grid cells are in progress and show previous mapping.